85-0292

Six Month Technical Report

TRANSIENT VELOCITY ASSESSMENT IN GALLIUM ARSENIDE, AND OF OTHER GaAs CHARACTERISTICS RELATED TO DEVICE FUNCTIONS

Sponsored by

Defense Advanced Research Projects Agency
ARPA Order No. 5020/1
Program Code 4D10

Contract No. MDA903-84-K-0374, issued by
Dep't. of the Army, Defense Supply Service,
Washington, DC 20310

Administered by ONR: Seattle
Serial RW-809

Scientific Program Officer: Mr. Sven A. Roosild, DARPA/DSO
1400 Wilson Blvd.
Arlington, VA 22209

Contractor: Oregon Graduate Center
19600 NW Von Neumann Dr.
Beaverton, OR 97006

Principal Investigator: J. S. Blakemore, Professor
Dep't. of Applied Physics and
Electrical Engineering
Phone: 503-690-1133

Contract Dates: August 29, 1984 - August 28, 1985

Reporting Period: August 29, 1984 - February 28, 1985

Report Submitted by:

J. S. Blakemore
Principal Investigator

R. E. Kremer
Faculty Associate

UNCLASSIFIED
SECURITY CLASSIFICATION OF THIS PAGE

REPORT DOCUMENTATION PAGE

1a. REPORT SECURITY CLASSIFICATION: UNCLASSIFIED	1b. RESTRICTIVE MARKINGS: NONE
2a. SECURITY CLASSIFICATION AUTHORITY	3. DISTRIBUTION/AVAILABILITY OF REPORT: Approved for Public Release Distribution Unlimited
2b. DECLASSIFICATION/DOWNGRADING SCHEDULE	
4. PERFORMING ORGANIZATION REPORT NUMBER(S): OGC - 71-521-SA-1	5. MONITORING ORGANIZATION REPORT NUMBER(S)
6a. NAME OF PERFORMING ORGANIZATION: Oregon Graduate Center; 6b. OFFICE SYMBOL (If applicable)	7a. NAME OF MONITORING ORGANIZATION: Office of Naval Research/Seattle
6c. ADDRESS (City, State and ZIP Code): 19600 NW Von Neumann Drive, Beaverton, Oregon 97006-1999	7b. ADDRESS (City, State and ZIP Code): 315 University District Building, 1107 NE 45 Street, Seattle, WA 98105
8a. NAME OF FUNDING/SPONSORING ORGANIZATION: Defense Advanced Projects Research Agency; 8b. OFFICE SYMBOL (If applicable)	9. PROCUREMENT INSTRUMENT IDENTIFICATION NUMBER: MDA903-84-K-0374
8c. ADDRESS (City, State and ZIP Code): 1400 Wilson Boilevard, Arlington, VA 22209	10. SOURCE OF FUNDING NOS.

PROGRAM ELEMENT NO.	PROJECT NO.	TASK NO.	WORK UNIT NO.
ARPA Order 5020/1		Program Code 4D10	

11. TITLE (Include Security Classification): Transient Velocity Assessment in GaAs (Unclassified)

12. PERSONAL AUTHOR(S): J. S. Blakemore and R. E. Kremer

13a. TYPE OF REPORT	13b. TIME COVERED	14. DATE OF REPORT (Yr., Mo., Day)	15. PAGE COUNT
Semi-Annual Technical	FROM 84/8 TO 85/2	85-6-10	41

16. SUPPLEMENTARY NOTATION: NONE

17. COSATI CODES		
FIELD	GROUP	SUB. GR.

18. SUBJECT TERMS (Continue on reverse if necessary and identify by block number): Gallium arsenide, submicron devices, ballistic transport, velocity saturation, semiconductor substrate evaluation, semi-insulating materials, electron defect evaluation

19. ABSTRACT (Continue on reverse if necessary and identify by block number)

Reports on the first six months of the program, with four tasks in two general areas. Concerning submicron GaAs devices and the possibility of high speed operation by velocity overshoot or ballistic mechanisms, tasks were to assemble the pertinent literature (now essentially done), and evaluate this - on which an interim evaluation is provided in the report to the effect that newly recognized scattering mechanisms make ballistic transport unlikely unless electron transit distances can be made less than some 100 nm. This looks more feasible with vertically-oriented devices. The other two tasks were an assessment of literature and information concerning EL2 and other significant defect states in GaAs (for which a substantial data base has been assembled), and participation in collaborative activities directed towards optimization of evaluation techniques for GaAs wafers to be used for FET and related integrated circuit purposes. Work to date indicates that the the local population of the EL2 midgap donor is likely to have a direct effect on FET properties.

20. DISTRIBUTION/AVAILABILITY OF ABSTRACT	21. ABSTRACT SECURITY CLASSIFICATION
UNCLASSIFIED/UNLIMITED ☒ SAME AS RPT. ☐ DTIC USERS ☐	UNCLASSIFIED

22a. NAME OF RESPONSIBLE INDIVIDUAL	22b. TELEPHONE NUMBER (Include Area Code)	22c. OFFICE SYMBOL
Sven A. Roosild	202-694-3010	DARPA/DSO

DD FORM 1473, 83 APR — EDITION OF 1 JAN 73 IS OBSOLETE.

UNCLASSIFIED
SECURITY CLASSIFICATION OF THIS PAGE

Transient Velocity Assessment in Gallium Arsenide,
and of other GaAs Characteristics Related to Device Functions

Table of Contents

TRANSIENT VELOCITY ASSESSMENT IN GALLIUM ARSENIDE, AND OF OTHER GaAs CHARACTERISTICS RELATED TO DEVICE FUNCTIONS

Six Month Technical Report

Executive Summary

Our efforts on this project can be divided into four broad areas:

A. Collection and assessment of literature dealing with experimental and theoretical work on high electronic velocity in GaAs material and devices.

B. Critique of the assumptions used in the theoretical work mentioned above.

C. Collection and assessment of data from the literature and our own lab concerning the midgap level EL2.

D. Using the EL2 data mentioned above to assess the quality of GaAs wafers as substrates for device purposes.

A. We have accumulated a large library of publications dealing with various aspects of carrier transport in GaAs. From this initial pool of about 250 articles, over 80 are concerned with velocity overshoot, ballistic transport, hot carrier response, etc. in a variety of materials. Bulk GaAs, two-terminal devices such as N+N-N+ diodes, and three-terminal devices (such as MESFETs and bipolar transistors) are treated. We have chosen to concentrate primarily on the three-terminal device literature.

B. As the dimensions of GaAs devices shrink, charge carriers

require less time to traverse the active region. For very short channels in a MESFET, for example, the transit time may be so short as to become comparable to the time between collisions for the electron. If the electron does not suffer any collisions during its trip through the channel, it is not likely to be scattered out of the gamma conduction band and into either the X or L bands, both of which give the electron a greater effective mass, and thus smaller mobility. Any theoretical work modeling the behavior of carriers in short-channel devices must be cognizant of this fact. Drift and/or diffusion transport equations must be incorporated into the model and statistical, collision-based equations such as the Boltzman transport equation must be used with care. The various scattering mechanisms influencing carrier transport need to be studied in detail. In addition to the "normal" scattering processes, "new" mechanisms seem to pop up regularly, as the rather rosy theoretical predictions are increasingly running up against far less optimistic experimental data. It may be that subpicosecond transit times for an electron in an FET are simply not possible. An analysis of the available literature indicates that the scattering distance is likely to be no more than 100 nm or so, which would make the resolution requirements for lithography almost intolerable for a device (MESFET, MODFET, etc.) in which carriers travel parallel to the surface plane. Accordingly it is necessary for us to examine the literature and status of vertically-oriented devices.

C. On a separate (materials dominant) topic also of concern for fast GaAs devices and ICs, we have been making a collection of information concerning the various midgap defect levels in GaAs, notably the "EL2" center. Our library on this and related topics currently contains over 400 articles and more are being added each week. As an indication of the still increasing amount of interest on this topic, over a fourth of the articles have release dates in 1984 or thus far in 1985. Even with all this activity, the microscopic nature of EL2 still remains an open question. It is widely considered that an antisite defect (As on a Ga site) is involved, but it has yet to be conclusively proven whether the antisite alone is responsible, or whether EL2 is a complex made up of the antisite plus one or more nearby defects. If a complex of some sort is eventually implicated, it is even more unclear as to what specific defects are involved. Published work, and oral presentations at various meetings through early 1985 do not indicate that the total identity of EL2 is close to reaching consensus status. This is, of course, a matter for concern since a continuing reliable commercial availability of "undoped LEC" GaAs is an essential for the GaAs IC industry to grow as planned.

D. Our work also concerns experimental measurements pertaining to EL2 and other midgap defects in GaAs. (Much of this experimental work is being carried out under NSF sponsorship, but on a

subject of simultaneous interest to DARPA.) These measurements include the mapping of the "neutral EL2 " concentration across the area of a GaAs wafer from infrared transmittance data. Our experimental technique has been developed in sensitivity to be able to make such measurements with a wafer (polished both sides) of nominal 0.5 mm thickness. Among the measurements of this kind that have been made to assist DARPA contractors have been transmittance maps on full wafers, part wafers, and thicker wafer slabs, sent to us by ARACOR, Inc. Some of these had been polished and partly thinned by the ARACOR "non-contact polish" technique. Measurements with this material were complicated in some cases by a lack of flatness for the treated surfaces; however, our assessment of ARACOR-treated material ends up as a finding that this treatment does <u>not</u> have any detectable effect on the EL2 concentration, as inferable from the optical transmittance. In collaboration with Tektronix/Triquint Semiconductors (another DARPA contractor), we have also conducted tests of comparisons among wafer maps of EL2, dislocations, and FET parameters. An initial stage of this work indicates an apparent correlation between the EL2 concentration and FET properties, as distinguishable from any effects of dislocations. This work is continuing.

Six Month Technical Report - Narrative

We now discuss each of the program areas in some detail, again dividing the project into the same four topics.

A. Collection and assessment of literature concerning high electronic velocity in GaAs. Much of the time in the initial phase of this project was spent gathering a base of literature dealing with transport in GaAs in general and with high electronic velocities in particular. While many of the articles deal with ballistic effects in bulk material, others treat the problem in a variety of both two- *and three-terminal* devices. The information gathered about the behavior of electrons in the bulk material can often be applied directly to electrons in the devices. In order to exploit the ballistic effects, the device geometries under consideration are very small. Since it is still quite difficult to fabricate MESFETs with 0.25 micron channels, most of the work published to date is theoretical in nature, often consisting of Monte Carlo simulations of electronic behavior. Our own effort has been narrowed to the assessment of the literature dealing primarily with three-terminal devices. The effects with which we are concerned are discussed in section B below, initially from a simplistic tutorial viewpoint, and then with recent pertinent literature as the basis for discussion.

B. Critique of the assumptions used in modeling ballistic

effects in three-terminal GaAs devices. Before providing a critique of the assumptions used in the modeling approaches, we need first to discuss the physical situation in short-channel devices and ascertain which assumptions would be appropriate. We will first discuss the topic of electronic transport in bulk GaAs and then study the additional effects caused by restraining the electronic motion to small spatial areas.

B.1 Scattering Mechanisms

Although some work has been done on hot hole transport in GaAs, we will concern ourselves here with electronic transport only. The conduction band in GaAs (shown in Fig. 1) is characterized by a direct minimum at the gamma point and two higher level valleys, the X band in the [100] direction and the L band in the [111] direction. Although it had earlier been thought that the X band was lower in energy than the L band, work in the mid-1970s (see the review [1]) has shown that the two bands are at a similar energy, with the L band actually being slightly lower. So while it is most favorable energetically for electrons to be in the gamma band, scattering processes and the application of large electric fields can cause large fractions of the electronic population to reside in the L and X valleys. The consequence of having electrons in these higher valleys can be seen by looking at the curvature of the bands in question in Fig. 1. The central minimum or gamma band is sharply curved leading to an electronic effective mass of only 0.063 m, where m is the mass of a free electron, while the less curved L and X

bands have effective masses of 0.222 m and 0.58 m respectively. Thus the mobility of electrons is greatly reduced when they get scattered from the gamma band to either of the other two. The key to having very high electronic velocities in GaAs is then, well recognized as being a mandate, to keep as large a fraction as possible of the electronic population in the gamma band for as long as possible.

There are two principal mechanisms for interband transfer of electrons. Since the L and X valleys are at higher energies than the gamma band, energy must either be added to the electron or the kinetic energy of the electron utilized. In any type of device, the electrons will be under the influence of an electric field. The effect of such a field on the population of the upper valleys is shown in Fig. 2 and the net effect on the electronic velocity is shown in Fig. 3, both from the well-established literature of "retrograde electron velocity" in GaAs.

In addition to being boosted into the higher energy, lower mobility bands by the application of an electric field, electrons may also get there as a result of various scattering processes. These processes include collisions with acoustic phonons through the deformation potential, collisions with polar optic phonons, ionized impurity scattering and nonpolar optic phonons [2], as well as other mechanisms. Indeed, it has been the case so far, that new scattering mechanisms are being uncovered at a rate that corresponds very well with the rate at which the experimental results are failing to live up to the theoretical predictions!

In order to properly model the behavior of electrons in devices it is necessary to include all of these scattering processes in the equations governing the electronic behavior. We have been increasingly finding that the "known" mechanisms have not been adequately describing the behavior found in the small amount of experimental work that has been done. "New" scattering processes, primarily dealing with electron-electron interactions, keep being proposed to explain the data.

Obviously, if the goal is to have the electron traverse the active region of a device before it is scattered or otherwise excited into the higher level valleys, one of the keys is to make the active region as short as possible. With the advances in technology that are currently being made, FETs with 0.25 micron channel lengths are no longer unfeasible. The rationale is to make the channel region so short that the electron does not have time to scatter while it is in the region. If the electron can cross the region without undergoing any collisions, it will be moving ballistically and may thereby attain a maximum velocity. Statistical treatments such as the Boltzmann Transport Equation (BTE) are based on the assumption of a large number of collisions during electronic transport. Drift and diffusion equations also take into account scattering and must be modified if they are to be used with any hope of accuracy.

Before we get into a specific critique of the assumptions used by various researchers, we will show a simple calculation designed to illustrate the times and speeds involved. Consider

an electron traveling with constant velocity 2 x 10^7 cm/s through a channel of length 0.4 micron; the transit time is then some 2 ps. Alternatively, suppose an electron in GaAs is accelerated from rest by a field E = 3 kV/cm for a temporal impulse lasting 1 ps with no scattering; a distance of 0.4 micron is covered, with a final velocity of 8 x 10^7 cm/s. Thus any scattering process with a time between collisions of a few picoseconds will, in general, be important. Usually, the scattering mechanisms are discussed in terms of their effect on the electronic mobility rather than the collision time (see, e.g., [3]). It has long been thought that the most prevalent form of scattering at 300 K is polar mode scattering by optical phonons. In addition, ionized impurity scattering will become increasingly important as the number of impurities becomes larger (as may be the case in the active region of a device). Deformation potential scattering by acoustic phonons can also play some role at room temperature. These mechanisms are compared in Fig. 4. Besides these relatively well-known mechanisms, several other modes may be important. Intervalley phonon modes and piezoelectric modes may also be important, and recent work has shown that electron-electron and electron-plasmon scattering processes play a critical role in limiting electronic velocities.

In addition to the above discussion of scattering mechanisms, we need to mention one further constraint. The aspect of the literature that we will be primarily concerned with is that

of the velocity of electrons. There is a maximum value of the velocity which should be used to compare the projected velocities of electrons in either the models or the actual devices. The group velocity of electrons in a material is defined as (dw/dk). This can be written as (1/h)(dE/dk) which is (1/h) times the slope of the E(k) relationship. Thus, the greater the slope of the band (not the curvature), the higher will be the maximum velocity possible in the material. For GaAs, the maximum slope is in the central or gamma conduction minimum in the [100] direction as shown in Fig. 1. This corresponds to a velocity of 1×10^8 cm/s. Any projected or claimed velocities greater than this value must then be viewed with skepticism.

B.2 Maximum Electron Velocity

We now discuss some of the literature dealing with very high electronic velocity in GaAs, restricting ourselves primarily to three-terminal devices. Two broad groups of theoretical models exist that discuss large velocity effects in GaAs. The first are Monte Carlo techniques based on the behavior of a large ensemble of electrons. The motion of the electrons is modeled as a sequence of free flights between collisions. Between collisions, the electrons are assumed to obey classical laws of motion determined by the band structure of the material. Collisions are considered to be random events, whose probabilities are known functions of energy. The duration of a free flight, the kind of scattering process and the change in momentum produced by the collision are determined by randomly produced numbers. This

gives, in essence, a numerical solution of the Boltzmann transport equation. The second group of models is based on a hydrodynamic interpretation of the Boltzmann transport equation, and involves much less computer time than do the Monte Carlo techniques. The second group are analytical rather than numerical. This group basically solves Poisson's equation with the appropriate boundary conditions using a fast Fourier transform. To be physically meaningful, the mesh spacing must be small enough to resolve the variation of the physical quantities involved. The fast Fourier transform is an iterative process and convergence is usually taken to occur when the solution for the potential changes by less than (kT/q). The models can be used to calculate various physical quantities of interest.

One of the earliest calculations of high electron velocity in GaAs was that by Ruch in 1972 [4]. His Monte Carlo method assumed that the dominant scattering mechanism was by polar optic phonons and also included the effects of acoustic phonons, non-parabolicity of the conduction band minimum and intervalley scattering through the admixture of p-type states. He concluded that the electrons would reach a maximum velocity of 4.7×10^7 cm/s and thus should be able to cross a 0.35 micron gate in about 1 ps. The electrons he injected were postulated to be cold, i.e., not excited before injection.

Other early work [5-7] made similar rosy predictions. The Monte Carlo simulations of Rees et al. [5] stated that velocities on the order of 2×10^7 should be possible for devices with

source-drain distances as long as 3.8 microns if the material is cooled to 80 K. Carnez et al. [6] mentioned that fringing effects due to the surfaces and the contacts need to be considered. Using pulsed fields, they claimed that for gate lengths of 0.3 micron, electrons could reach velocities of 8×10^7, with velocities of 3×10^7 possible for steady state conditions. Shur and Eastman [7] discussed the possibility of injecting the electrons with a considerable energy and thus not having to accelerate the electrons in the gate region. To prevent intervalley transfer, they limited the injection energy to 0.35 eV, the energy difference between the gamma and L bands. For a device operating at 77 K, they inferred that ballistic transport is certainly possible and should provide velocities in the mid 10^7 range.

The first experimental evidence of ballistic motion in a three terminal device was provided by Eastman et al. [8] in 1980. They said that the mean free path between collisions was limited by polar optical phonons to about 0.1 - 0.2 microns. Since their device structure had a length of 0.5 microns, they assumed that the electrons suffered two or three collisions during the transit. Their electron flow showed definite evidence of being partially-ballistic in nature rather than showing saturation.

These optimistic predictions continued for the next couple of years with no real experimental confirmation [9-16]. Most of the velocities estimated from the models mentioned above were in

the mid 10^7 range. The first real note of caution came in 1980 by Barker et al. [17,18]. They correctly pointed out that with gate lengths on the order of 0.25 micron, the thickness of the layer was no longer negligibly small. Instead of a one-dimensional problem, one had to work in two dimensions. In addition to surface scattering, which had been generally ignored, they claimed that the electron flow may actually be space-charge limited. Coulombic electron-electron interactions could play a vital role in the scattering process. Their conclusion was that the boundary conditions were what dominated the electronic motion, not ballistic effects. Thus, by simply studying the I-V characteristics of short devices, ballistic effects could not even be observed.

One of the few experimental papers of 1981 provided some information that could be taken as either incouraging or discouraging. Shank et al. [19] used a subpicosecond optical technique to measure the electron dynamics in a two-terminal diode made of AlGaAs on GaAs. To fit their data, they assumed an electron velocity of 4.4×10^7 for the first 1.1 picoseconds of the electron's travel between the contacts and then a slower 1.2×10^7 for the rest of the crossing. This information was encouraging in that it was the first direct confirmation of electronic velocity significantly greater than 10^7, but discouraging for several reasons. First, it took place in a AlGaAs-GaAs heterostructure rather than in GaAs. Second, the short period of rapid transit corresponded to a length of only about 0.2 micron and

most importantly, the experiment took place at 77 K rather than at room temperature.

The Cornell group still maintained that by injecting electrons that were already ballistic (velocity = 1×10^8), very large speeds could be maintained for as long as 0.3 micron. In fact, even assuming gradual acceleration, they claimed speeds reaching 5×10^7 for lengths of 0.3 micron. Their model considered only polar optical scattering and allowed injection energies of up to 0.36 eV with no intervalley scattering.

In the last couple of years, however, the theoretical work has shown much less optimism. Although some models still predicted fairly high velocities (the hydrodynamic model of Buot and Frey claimed that $v = 3.8 \times 10^7$ was possible for a .25 micron gate [21], and a one-dimensional model developed by Shukhanov et al. claimed 6×10^7 cm/s [22]), the Monte Carlo studies were finding that other mechanisms, (previously ignored) caused the path length where the velocity was rapid to shrink very rapidly. Littlejohn et al. [23] found that even if the average injection energy of electrons was less than 0.36 eV, (i.e., the intervalley energy) enough electrons have greater energies so that intervalley scattering is very important. Ballistically launched electrons lose their momentum very rapidly (on the order of a few hundred angstroms), rather than slowly over about 0.3 microns as previously expected. For base widths of about 250 angstroms, velocities as high as 4×10^7 cm/s may be possible, but for lengths of 0.1 micron, speeds only half that fast can be

maintained. Awano et al. [24] painted a somewhat brighter picture, claiming a velocity of 7×10^7 at a distance of 0.16 microns from the source. The device they model has both the gate and the source-drain distance equal to 0.25 micron. They include intervalley scattering and collisions with ionized impurities. A more detailed work by the same group [25] claims that the electrons are accelerated very rapidly (in the first 0.02 micron or so) up to speeds of 3.5×10^7 cm/s and then more slowly up to about 8.5×10^7 over the remainder of the .25 micron source-drain length. They claim that some electrons may even reach velocities of 1.2×10^8 cm/s. The fact that this value is faster that the physically allowed maximum velocity in GaAs causes one to doubt the veracity of their work! In addition, the above-quoted values of velocity were for a temperature of 77 K rather at room temperature, so their usefulness is further undermined. Their calculations do reveal one interesting phenomenon - namely that charge tends to pile up at the drain end of the channel. This increase in charge density (shown in Fig. 5) could lead to stronger electron-electron interactions, although Awano et al. did not include any scattering mechanisms of this type in their calculation.

The Cornell group has been the primary group publishing experimental results in the last couple of years [26,27]. They found that the predictions based on polar optical phonon scattering being the most important mechanism were overly optimistic. The devices they were building did not perform up to the predic-

tions. In fact there tended to be a more than two to one discrepancy. In order to explain the discrepancy, Hollis et al. [26] postulated several new scattering mechanisms. They had previously neglected electron-electron scattering and scattering from coupled plasmon-optical phonon modes. Compared to the previously considered primary scattering mechanism, the polar optical phonon scattering, they found that the electron-electron scattering had a rate that was larger by more than 30 percent and that the plasmon-phonon modes accounted for more than twice as much scattering as the polar modes. Without these extra scattering modes present, the Monte Carlo simulations provided device parameters that were approximately twice as optimistic as the actual performance. Recognizing the limits these new scattering mechanisms place on device geometries, the Cornell group is no longer working on the standard MESFET. Their planar-doped barrier transistor is a vertically oriented device that uses a barrier to inject electrons with a couple of tenths of an eV energy (corresponding to velocities in the upper 10^7 cm/s). This vertical geometry allows them to have base lengths that are very short. The work of Hollis et al. [26] dealt with base widths from 700 - 2000 angstroms. This work has been detailed more thoroughly here because it seems to present a good possibility for high speed devices, as will be discussed below.

Very recent studies have tended to confirm the Cornell results. Monte Carlo studies by Lugli and Ferry [28] have shown that electron-electron and electron-plasmon interactions severely

limit the possibility of ballistic transport except for very short distances. Even working at energies low enough that plasmon-phonon coupling and intervalley scattering can be neglected, they found that the Coulombic interactions mentioned above cause the electronic velocity to fall to about half of its injected value after only 1000 - 2000 angstroms, as shown in Fig. 6. Work by Hayes et al. [29] also found strong electron-electron scattering. Assuming that this mechanism is equally strong as the LO phonon scattering, their Monte Carlo results gave a scattering length of 400 angstroms. They did not include coupled plasmon modes or impurity scattering in their model. Experimental work by the same group [29] injected electrons with 0.25 eV into devices with base lengths of 1200 and 1700 angstroms. They found that the electrons experience considerable scattering during the transit of the base, with, as expected, electrons in the 1700 angstrom base being scattered more than in the 1200 angstrom base. Finally, Chen et al. [30] have recently measured velocities of about 2×10^7 cm/s in InGaAs devices and suggest that this could be speeded up somewhat by using InGaAs devices with gates made of GaAs. This latter type of device has yet to be fabricated.

What we have found, therefore, is that as the fabrication technology is improved and actual devices are being made, the results are considerably less rosy than the early predictions of a few years ago. With the large number of electrons present in the active regions of most devices, the flow tends to be space

charge limited and Coulombic interactions between electrons and plasmons and among electrons themselves are the dominant scattering mechanisms. It appears to us that with the scattering lengths getting down into the few hundreds of angstroms range it will be increasingly difficult to fabricate standard geometry MESFETs with gate and/or channel lengths adequately small. The best chance for actually making devices with very fast switching speeds (at room temperature, of course) appears to lie in vertically oriented geometries, where the active regions may be easily made a few hundred angstroms thick. Figure 7 shows an energy diagram of the planar doped barrier transistor mentioned above. A second possibility that also allows for very short transit distances due to its vertical orientation is the permeable base transistor [31,32]. Its geometry is shown in Fig. 8.

C. Collection and assessment of literature concerning the midgap level EL2. As stated in the summary above, the amount of literature dealing with EL2 is quite astounding. Perhaps even more amazing, is that even with all the effort being applied to the problem, the exact physical nature of the defect remains unknown. Information gathered over the last two years has indicated that the defect likely involves an As on Ga antisite, but there is still some disagreement as to whether the isolated antisite alone is the culprit or whether it forms a complex with some other defect. The only real change in the situation over the last six months is that perhaps fewer people are touting the

isolated antisite as the mechanism responsible for EL2. It appears more and more likely that some other entity is also involved. However, there is still no consensus at all as to the identification of this other entity. One reasonable guess would be a nearby As vacancy, but other complexes have also been promoted. The status of the search for the identity of EL2 will be further described in out Fourth Quarter R & D Status report, and the Final Technical Report, these having the opportunity to include information reported during conferences in the summer of 1985.

D. Mapping of EL2, and Use of EL2 and Other Mapping Data to Assess the Quality of GaAs Wafers as Device Substrates. There has been much recent interest in measuring the properties of a GaAs wafer not just at one point, but at many locations - and the drawing of maps, for EL2 concentration, dislocations, luminescence, device properties, etc. A summary of papers appearing from 1982 to the beginning of 1985 on these related topics is provided as Appendix A of this report, on pages numbered A.1 and A.2. That Appendix lists over 50 papers that have appeared in that two-year period; and a number more such will appear in 1985, especially in view of the July 1985 symposium in Montpellier, France on Defect Recognition and Image Processing (D.R.I.P.) in III-V compounds.

Some of the studies by Japanese workers have led to reports from them [33,34] that the proximity of a dislocation to a FET

produces a direct shift of the threshold voltage, by up to 300 mV. This contrasts with reports from the Hughes Research group [35] that there was no direct dislocation/FET correlation in the wafers they studied. Are these reports conflicting? Or does each report spring from a limited source of information? Note that the EL2 concentration was not mapped in either of these studies. Thus our own work (much of this carried out under a program here supported by NSF) has attempted to obtain information about the mapping of EL2, dislocations, and device properties, all in the same wafer. Such a comparison is possible only using the highly refined technique we have developed for measuring the weak absorption of neutral EL2 despite having this dispersed only in a thin (0.5 mm) wafer. Figures 9 through 12 illustrate results obtained in our work, which show: there is a direct correlation between EL2 and device properties, and also, that the device pattern may resemble that of dislocations if the latter share that pattern also with the EL2 population. Thus a wafer for which lengthy post-growth anneal has permitted a dissolution of any original stress-induced coincidence of EL2 and dislocations is apt to have the device variations follow those of EL2 rather than dislocations. The subject is of such great importance that further work is essential.

References

1. J. S. Blakemore, J. Appl. Phys. 53, R123 (1982).
2. S. Kratzer and J. Frey, J. Appl. Phys. 49, 4064 (1978).
3. G. E. Stillman et al., J. Phys. Chem. Sol. 31, 1199 (1970).
4. J. G. Ruch, IEEE Trans. - Elec. Dev. ED-19, 652 (1972).
5. H. Rees et al., Elec. Lett. 13, 156 (1977).
6. M. S. Shur and L. F. Eastman, IEEE Trans. - Elec. Dev. ED-26, 1677 (1979).
7. B. Carnez et al., J. Appl. Phys. 51, 784 (1980).
8. L. F. Eastman et al., Elec. Lett. 16, 524 (1980).
9. A. A. Kastalsky and M. S. Shur, Sol. St. Comm. 39,715 (1981)
10. S. Laval et al., Inst. Phys. Conf. Ser. 56, 171, (1981).
11. W. R. Curtice and Y. H. Yun, IEEE Trans. - Elec. Dev. ED-28, 954 (1981).
12. J. A. Higgins and D. N. Pattanayak, IEEE Trans. - Elec. Dev. ED-29, 179 (1982).
13. J. V. Faricelli et al., IEEE Trans. - Elec. Dev. ED-29, 377 (1982).
14. T. Wada and J. Frey, IEEE J. Sol. St. Cir. SC-14, 398 (1979).
15. R. K. Cook and J. Frey, IEEE Trans. - Elec. Dev. ED-29, 970 (1982).
16. J. F. Pone et al., IEEE Trans. - Elec. Dev. ED-29, 1244 (1982).
17. J. R. Barker and D. K. Ferry, Sol. St. Elec. 23, 519 (1980), 23, 531 (1980), 23, 545 (1980).

18. J. R. Barker et al., IEEE Elec. Dev. Lett. EDL-1, 209 (1980).

19. C. V. Shank et al., Appl. Phys. Lett. 38, 104 (1981).

20. L. F. Eastman, Inst. Phys. Conf. Ser. 63, 245 (1982).

21. F. A. Buot and J. Frey, Sol. St. Elec. 26, 617 (1983).

22. A. A. Sukhanov et al., Sov. Phys. - Semicond. 17,1378 (1983).

23. M. A. Littlejohn et al., J. Vac. Sci. Tech. B 1, 449 (1983).

24. Y. Awano et al., Elec. Lett. 19, 20 (1983).

25. Y. Awano et al., IEEE Trans. - Elec. Dev. ED-31, 448 (1984).

26. M. A. Hollis et al., IEEE Elec. Dev. Lett. EDL-4, 440 (1983).

27. L. F. Eastman et al., Annual Rep't. to DARPA (1984).

28. P. Lugli and D. K. Ferry, IEEE Elec. Dev. Lett. EDL-6, 25 (1985).

29. J. R. Hayes et al., Phys. Rev. Lett. 54, 1570 (1985).

30. C. Y. Chen et al., IEEE Elec. Dev. Lett. EDL-6, 20 (1985).

31. C. O. Bozler and G. D. Alley, IEEE Trans. - Elec. Dev. ED-27, 1128 (1980).

32. W. R. Frensley, IEEE Trans. - Elec. Dev. ED-30, 1624 (1983).

33. S. Miyazawa et al., Appl. Phys. Lett. 43, 853 (1983).

34. Y. Ishii et al., IEEE Trans. - Elec. Dev. ED-31, 800 (1984).

35. H. V. Winston et al., Appl. Phys. Lett. 45, 447 (1984).

FIGURE CAPTIONS

1. Energy band structure of GaAs at 300 K from [1].
2. Fraction of electrons in the upper valleys and average electronic energy as a function of electric field from [15].
3. Electronic velocity as a function of electric field for silicon, InP and GaAs from [14]. In all cases, $N_D=10^{17}/cm^3$.
4. Scattering mechanisms considered in most early calculations as a function of temperature from [3].
5. Monte Carlo calculation from [25] showing the increase in carrier density near the drain end of the channel.
6. Recent calculation showing average drift velocity vs. distance both with (solid lines) and without (dashed lines) electron-electron interactions for two different injection energies from [28].
7. Energy diagram for the planar doped barrier transistor. The Emitter-Base junction is the hot electron injector, the Base is the transit region, and the Base-Collector junction acts as the hot electron analyzer. The dashed lines indicate the band edge under various biasing conditions. From [29].
8. Device geometry of the permeable base transistor from [31]. A tungsten grating is embedded in the GaAs and the electrons pass through slits in it.
9. Comparison of maps showing EL2 concentration, dislocation density and device parameters for wafer X, an undoped 50 mm

diameter GaAs wafer.

10. Comparison of maps for wafer Y, also an undoped, 50 mm diameter GaAs wafer.
11. Correlation plots for wafer Y relating FET properties to the neutral EL2 concentration.
12. Comparison of maps for wafer Z, an In-doped 50 mm diameter GaAs wafer.

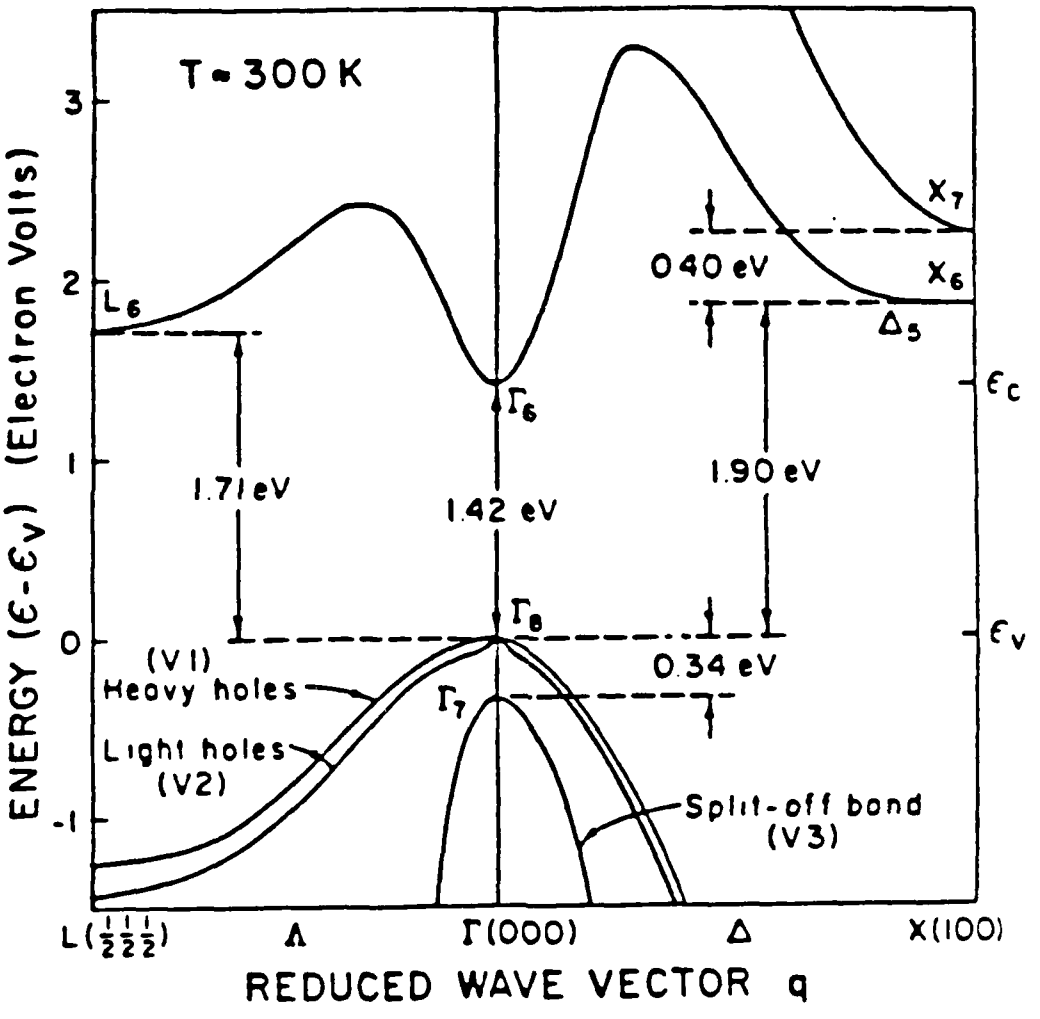
T = 300 K
ENERGY (ε-εV) (Electron Volts)
3
2
1
0
-1
L6
Γ6
X7
X6
Δ5
040 eV
εc
εv
1.71 eV
1.42 eV
1.90 eV
Γ8
0.34 eV
(V1)
Heavy holes
Γ7
Light holes
(V2)
Split-off bond
(V3)
L(½½½)
Λ
Γ(000)
Δ
X(100)
REDUCED WAVE VECTOR q

Figure 1

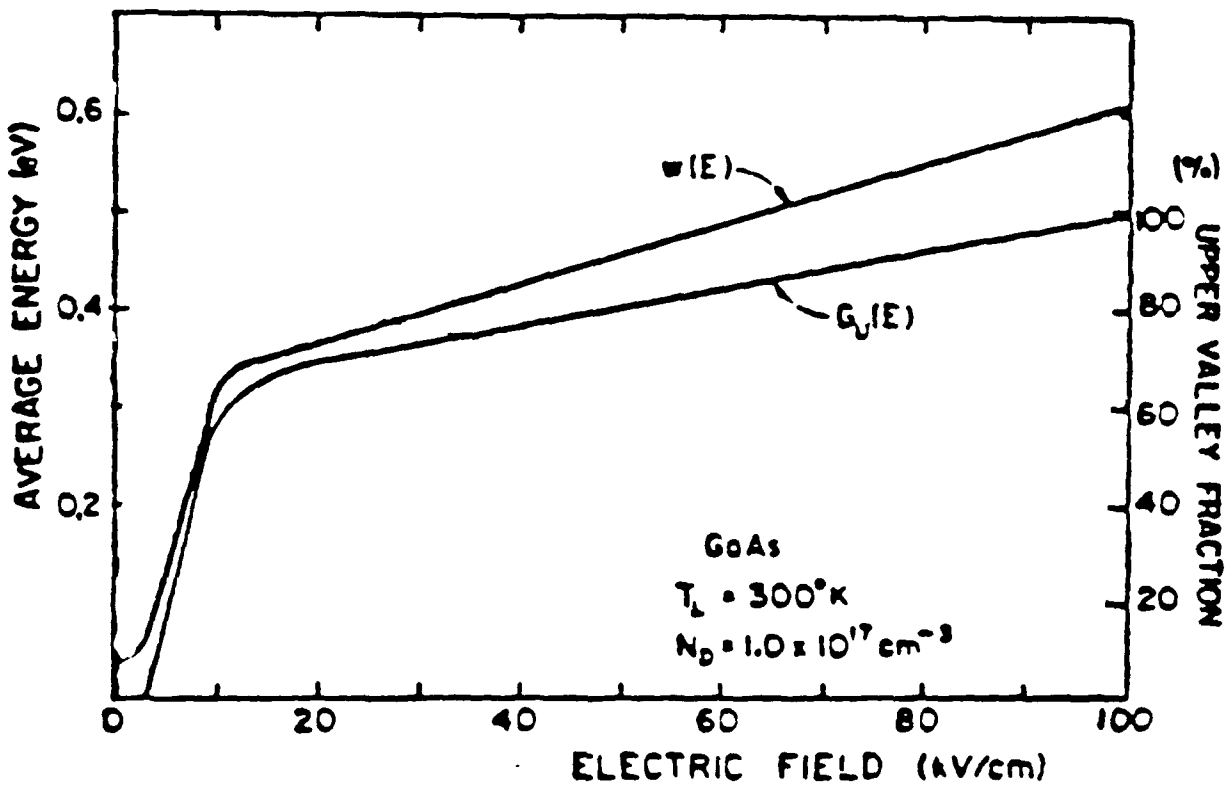
AVERAGE ENERGY (eV)
0.6
0.4
0.2
w(E)
$G_U(E)$
(%)
100
80
60
40
20
UPPER VALLEY FRACTION
GaAs
T_L = 300°K
N_D = 1.0 x 10^{17} cm^{-3}
0
20
40
60
80
100
ELECTRIC FIELD (kV/cm)

Figure 2

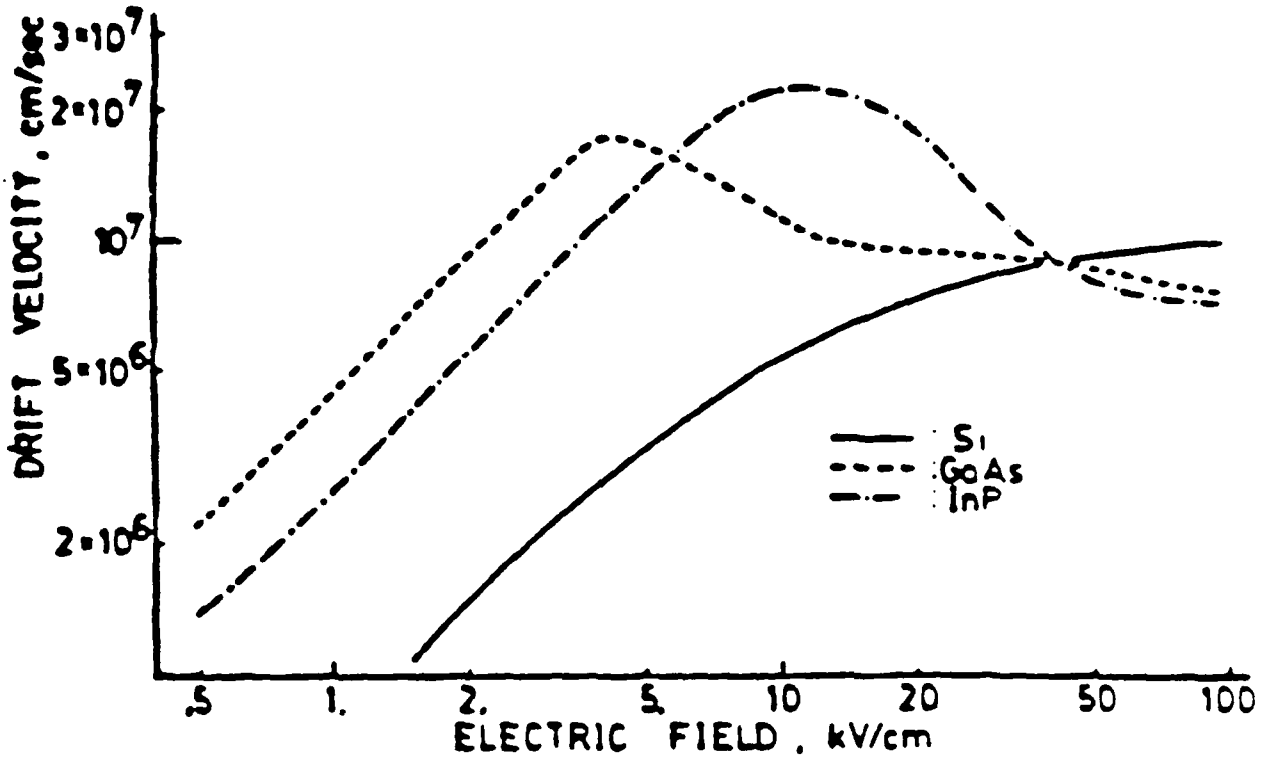
DRIFT VELOCITY, cm/sec
3×10^7
2×10^7
10^7
5×10^6
2×10^6
.5
1.
2.
5.
10
20
50
100
ELECTRIC FIELD, kV/cm
Si
GaAs
InP

Figure 3

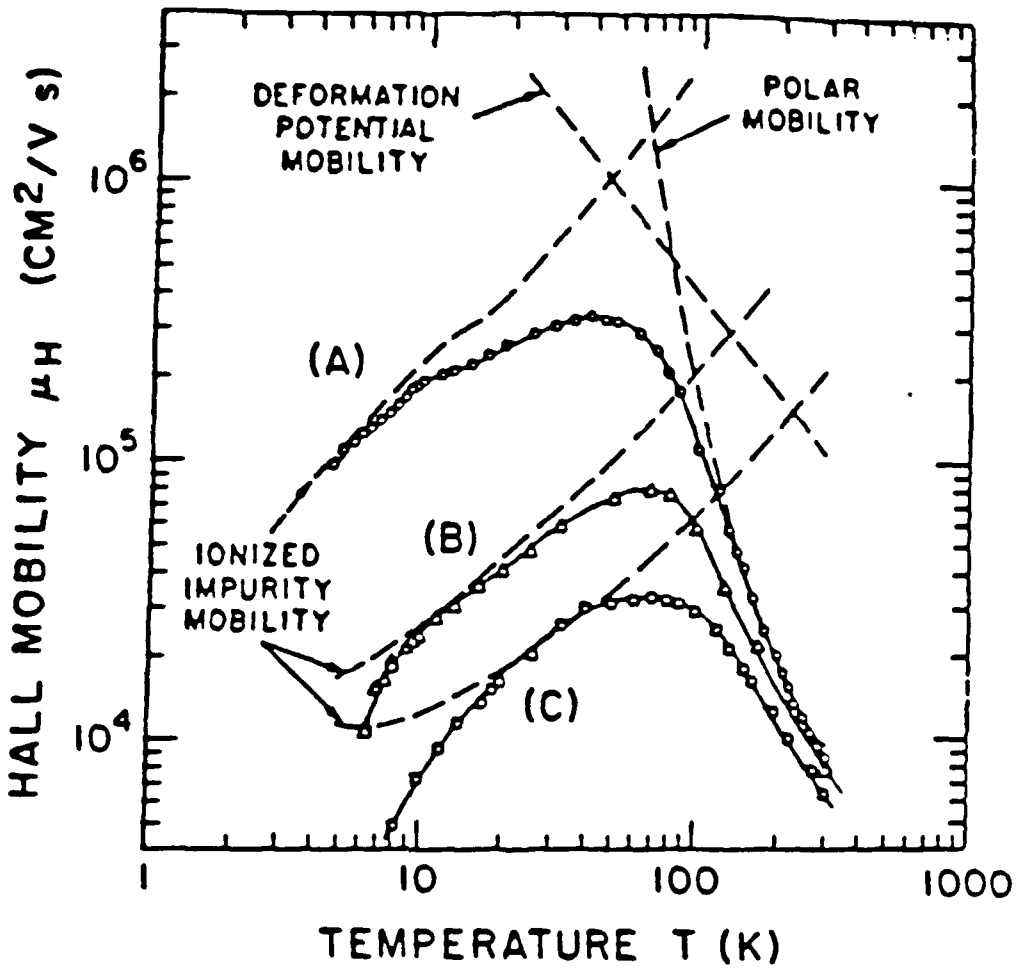
DEFORMATION POTENTIAL MOBILITY
POLAR MOBILITY
IONIZED IMPURITY MOBILITY
(A)
(B)
(C)
HALL MOBILITY μ_H (CM^2/V s)
10^6
10^5
10^4
1
10
100
1000
TEMPERATURE T (K)

Figure 4

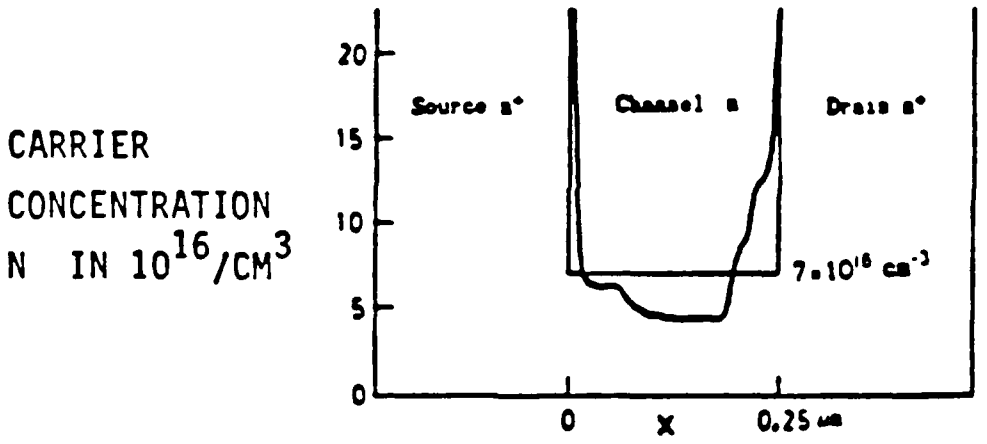
CARRIER
CONCENTRATION
N IN $10^{16}/CM^3$
20
15
10
5
0
Source n+
Channel n
Drain n+
$7 \cdot 10^{16}$ cm^{-3}
0
x
0.25 µm

Figure 5

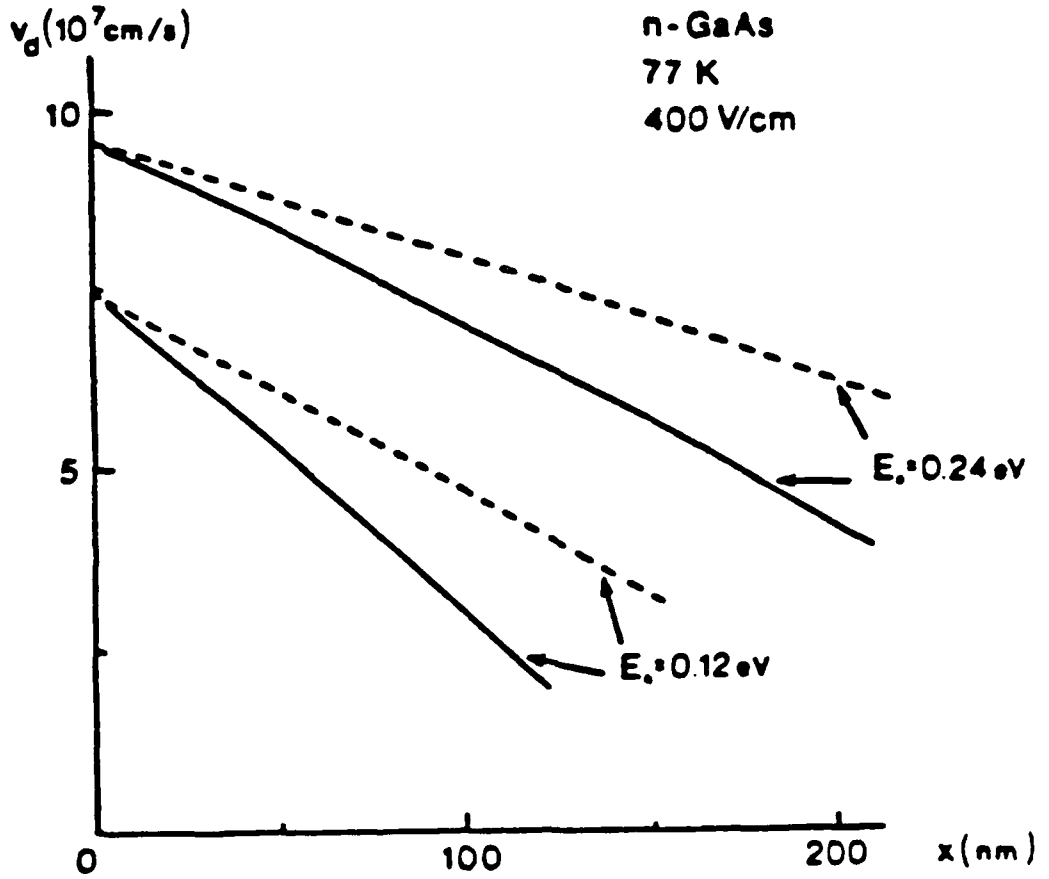

Figure 6

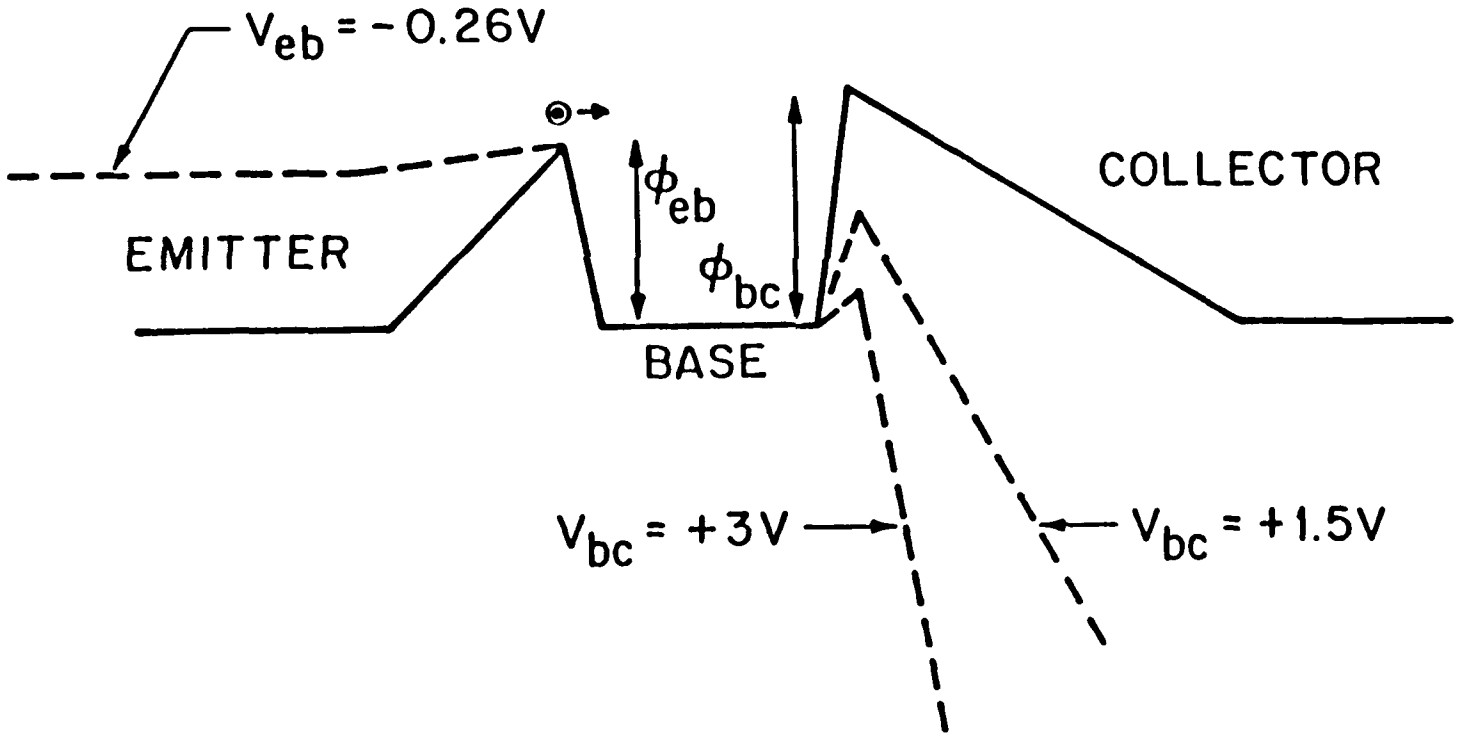

Figure 7

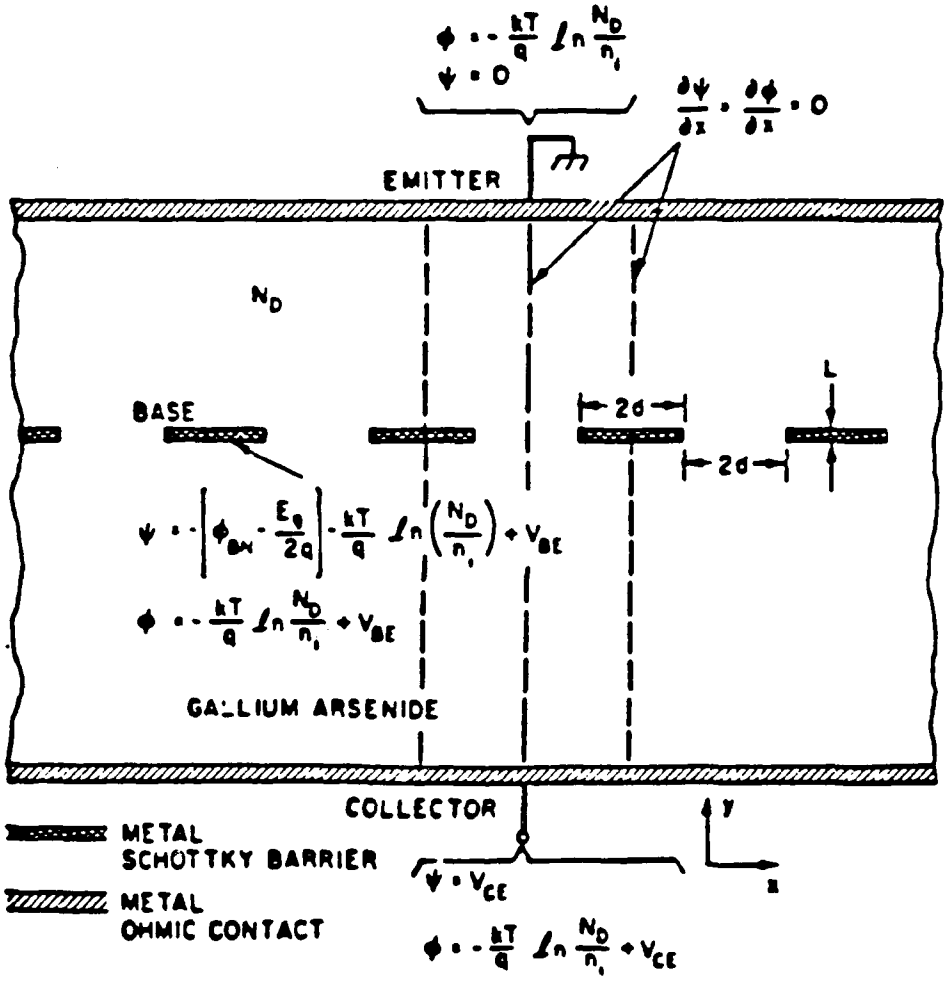
$\phi = -\frac{kT}{q} \ln \frac{N_D}{n_i}$
$\psi = 0$
$\frac{\partial \psi}{\partial x} = \frac{\partial \phi}{\partial x} = 0$
EMITTER
N_D
BASE
2d
L
2d
$\psi = -\left|\phi_{BN} - \frac{E_g}{2q}\right| - \frac{kT}{q} \ln\left(\frac{N_D}{n_i}\right) + V_{BE}$
$\phi = -\frac{kT}{q} \ln \frac{N_D}{n_i} + V_{BE}$
GALLIUM ARSENIDE
COLLECTOR
y
x
METAL
SCHOTTKY BARRIER
METAL
OHMIC CONTACT
$\psi = V_{CE}$
$\phi = -\frac{kT}{q} \ln \frac{N_D}{n_i} + V_{CE}$

Figure 8

COMPARISON OF SPATIAL DISTRIBUTIONS ACROSS WAFER "X"
("UNDOPED" S.I. GaAs, 50 mm DIAMETER, 0.5 mm THICK)
OF (a) NEUTRAL EL2 CONCENTRATION N°
(b) DISLOCATION DENSITY, N_D
(c) I_{dss} FOR MESFET DEVICES MADE IN THIS WAFER.

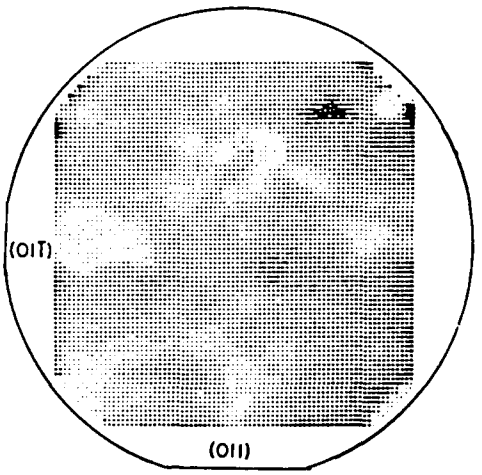

300 K NEAR-IR TRANSMITTANCE INDICATES $\bar{N}° = 1.1 \times 10^{16}\ cm^{-3}$ WITH ±10% DEVIATIONS, AND ⟨011⟩-ORIENTED MINIMA.

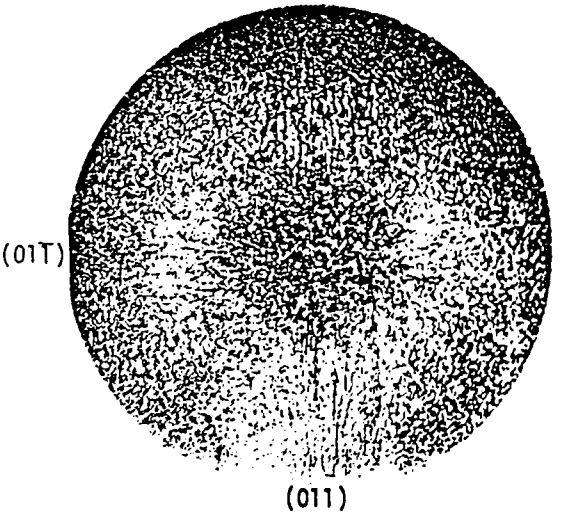

THE WAFER AFTER MOLTEN KOH ETCHING TO SHOW DISLOCATIONS, WITH 4-FOLD SYMMETRY, AND A RANGE $2 \times 10^4 < N_D < 7 \times 10^4\ cm^{-2}$.

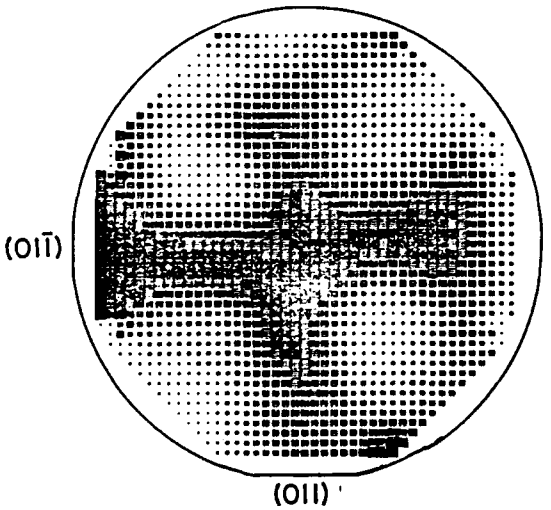

I_{dss} VALUES FOR MESFET ARRAY MADE IN WAFER "X". EACH STEP DARKER MEANS 1% RISE IN I_{dss}.

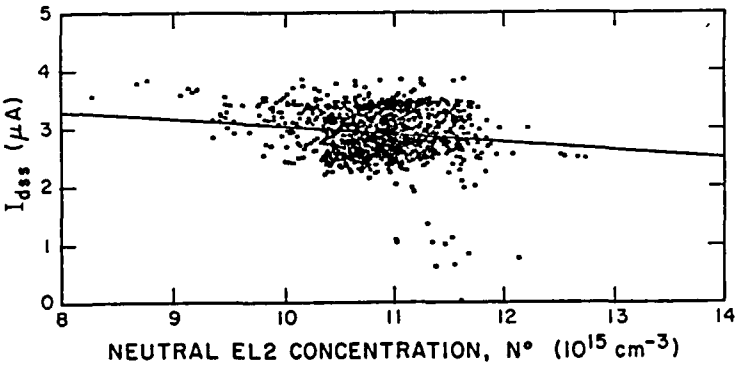

CORRELATION PLOT OF MESFET I_{dss} AGAINST BULK EL2 N°, WITH >99% SIGNIFICANCE. BUT SINCE WAFER "X" HAS ABOVE-NORMAL N° AND N_D WITH THE SAME 4-FOLD SYMMETRY, THIS WAFER CAN'T DISTINGUISH BETWEEN EL2 AND DISLOCATION PROXIMITY AS AFFECTING A FET.

Figure 9

COMPARISON OF MAPS FOR EL2 AND DEVICE PROPERTIES FOR WAFER "Y"

[THIS ALSO IS "UNDOPED" S.I. GaAs, 50 mm DIAMETER, 0.5 mm THICK. FOR THIS TAIL-END WAFER, N_D IS LARGE ($\sim 2 \times 10^5$ cm^{-2}) AND UNIFORM. THUS THE RADIAL VARIATION OF N° ("W-SHAPED" DIAMETER PROFILE), ALSO SEEN FOR I_{dss} AND V_{th} OF A MESFET, IS NOT MATCHED BY A COMPARABLE VARIATION OF THE DISLOCATION DENSITY FOR THIS WAFER.]

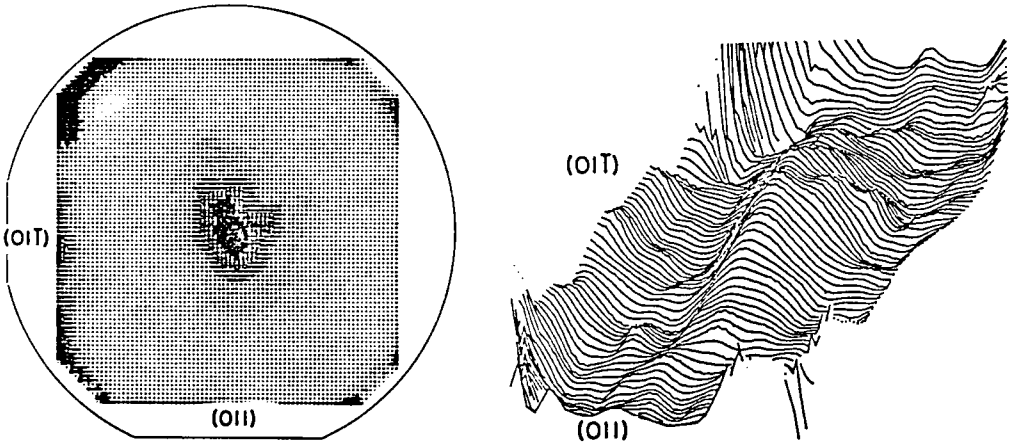

ABOVE, THE MEASURED EL2° DISTRIBUTION, WITH MEAN $\bar{N}° = 8 \times 10^{15}$ cm^{-3}, A "W-SHAPED" DIAMETER PROFILE WITH CENTRAL MAXIMUM SOME 20% ABOVE THE MEAN. (STEPS HERE ARE OF $\Delta N° = 3 \times 10^{14}$ cm^{-3}.)

BELOW, MAPS OF MESFET DEVICE PARAMETERS; I_{dss} AT THE LEFT, WITH EACH STEP OF DARKER SHADING DENOTING 1% LARGER CURRENT. V_{th} AT THE RIGHT, WITH EACH STEP OF MORE SHADING INDICATING THAT V_{th} HAS BECOME 7 mV LESS NEGATIVE.

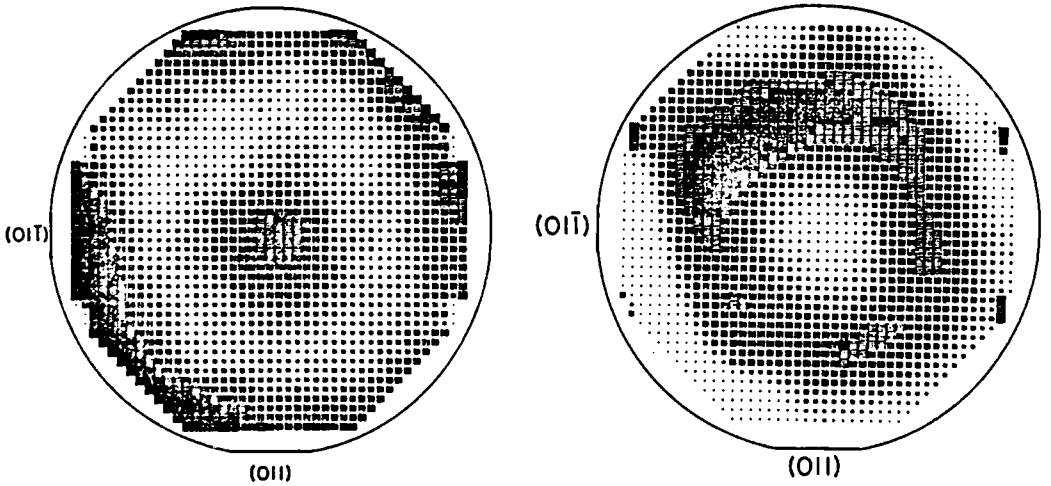

Figure 10

CORRELATION PLOTS FOR WAFER "Y". FET PROPERTIES vs. NEUTRAL EL2

THESE PLOTS TAKE DATA OF I_{dss} (UPPER FIGURE) OR V_{th} (LOWER FIGURE) FOR THE MESFET ARRAY CREATED ON A 1 x 1 mm^2 GRID ACROSS THE WAFER, CORRELATED WITH N° MEASURED AT THESE LOCATIONS. THUS EACH COMPRISES ABOUT 1600 DATA POINTS; AND THE CONFIDENCE LEVEL IS >99% FOR EACH.

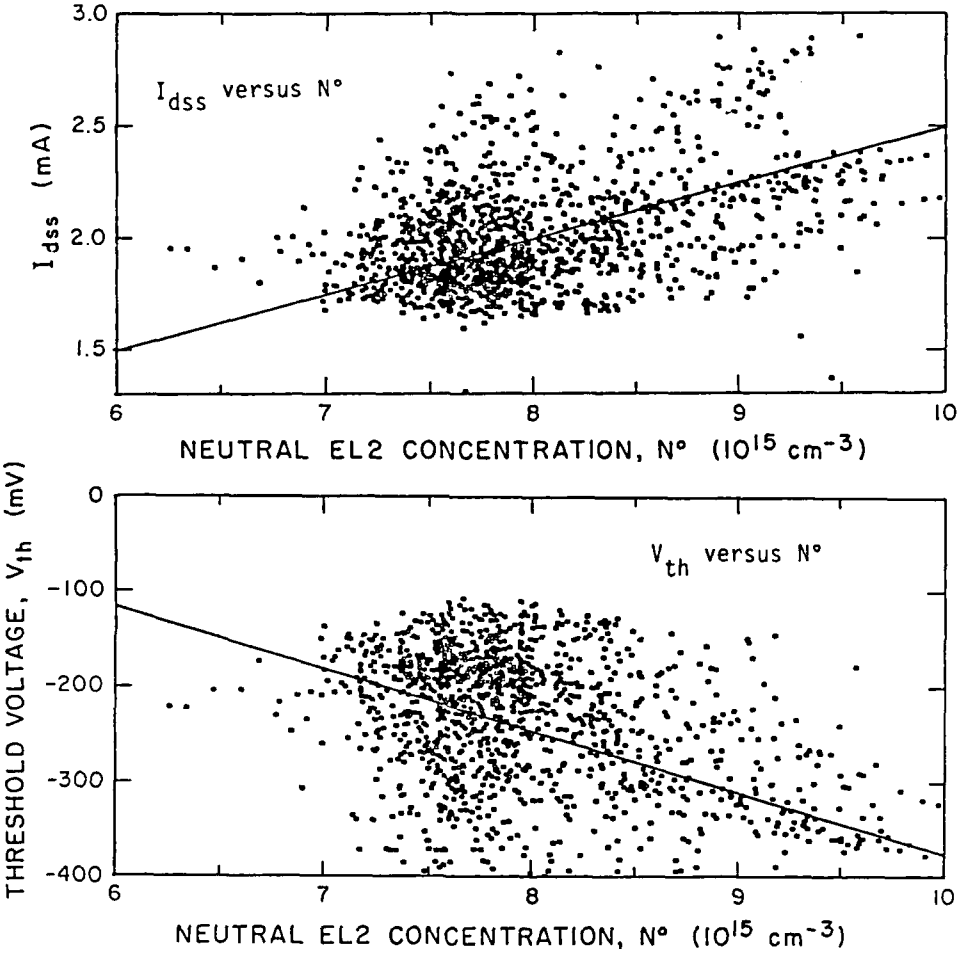

SINCE THE DISLOCATION DENSITY N_D, WHILE LARGE FOR THIS WAFER WAS ALSO SPATIALLY UNIFORM, THE DATA POINT TOWARDS A DIRECT INFLUENCE OF THE EL2 CONCENTRATION IN THE STARTING SUBSTRATE ON THE CHANNEL CONDUCTANCE — INFLUENCED PRESUMABLY BY THE EL2 COMPONENT OF THE SPACE CHARGE AT THE CHANNEL/SUBSTRATE INTERFACE. WE SEE EVIDENCE OF EL2 AT THAT INTERFACE FROM OUR PHOTOFET AND SIDE-GATE EXPERIMENTS, AS WELL AS DEEP-LEVEL STATES WHICH ARE RESIDUES OF IMPLANT DAMAGE.

Figure 11

COMPARISONS OF EL2 CONCENTRATION, DISLOCATIONS, AND FET PROPERTIES FOR INDIUM-DOPED LEC S.I. WAFER "Z". [ALSO 50 mm DIAM, 0.5 mm THICK]

INDIUM DOPING IS BEING EXPERIMENTED WITH IN LEC GROWTH OF S.I. GaAs TO "HARDEN" THE LATTICE AND REDUCE DISLOCATION DENSITY — HOPEFULLY TOWARDS ZERO. IN THE PRESENT CASE, EVIDENTLY THERE WAS NOT ENOUGH In INCORPORATED, AND $N_D \neq 0$. AN X-RAY TOPOGRAPH (COURTESY OF DICK FORMAN OF NBS) SHOWS A FOUR-FOLD N_D DISTRIBUTION WITH CENTRAL MAXIMUM

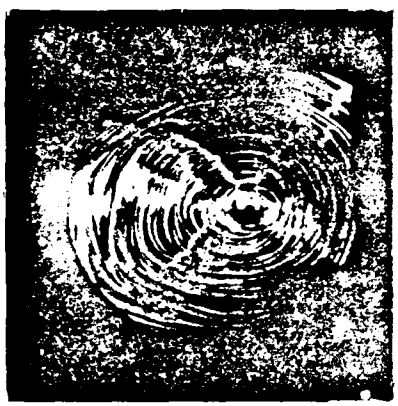

XRT PICTURE OF DISLOCATIONS, WITH CENTRAL MAXIMUM VALUE $N_D \sim 10^4$ cm^{-2}.

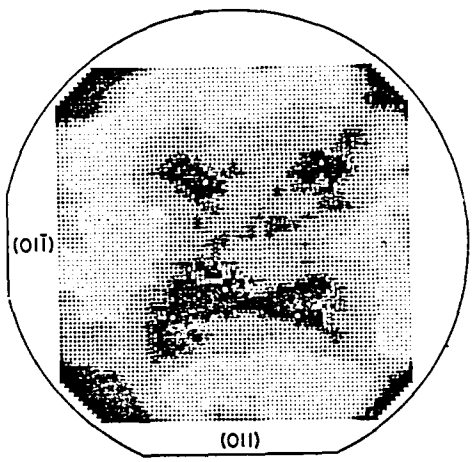

THE EL2 DISTRIBUTION, AVERAGING $\bar{N}° = 6 \times 10^{15}$ cm^{-3}, FOUR-FOLD SYMMETRY WITHOUT CENTRAL MAXIMUM.

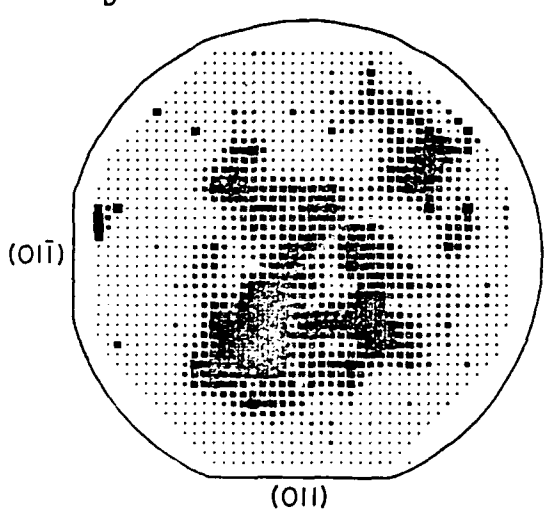

DISTRIBUTION OF V_{th} VALUES FOR FETs MADE IN ADJACENT WAFER Z'. MEAN IS $\bar{V}_{th}$ = +600 mV, WITH TEN STEPS OF ΔV_{th} = 10 mV.

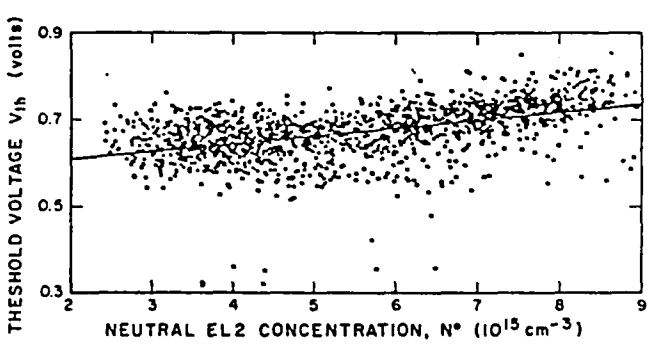

CORRELATION BETWEEN FET THRESHOLD VOLTAGE VALUES FOR THE MESFETS OF WAFER Z', WITH OPTICALLY MEASURED EL2 N° IN THE ADJACENT WAFER Z.

Figure 12

APPENDIX A

LITERATURE, SINCE 1982, CONCERNING WAFER SCANNING/MAPPING OF SEMI-INSULATING GaAs 'WAFERS'. SUMMARIZED THROUGH FEBRUARY 1985

(Note that many samples from the first section, EL2, are several mm thick, thus are not true 'wafers'.)

Papers Reporting on the Spatial Variation of the EL2 Concentration in S.I. GaAs Wafers, from IR Transmission

Authors	Published Conference or Journal	Publication Date	Type of Crystal	Diameter (mm)	Thickness (mm)	Other Material Features	Form of Data Presentation
Holmes et al	Evian Conf.	1982	LEC (HP)	75	4		Radial line plot
Holmes et al.	A.P.L.,	3/83	LEC (HP)	75	4		Radial line plot
Brozel et al.	A.P.L.	4/83	LEC (HP)	50	5		Radial line plot; also vidicon micrograph
Holmes et al.	A.P.L.	8/83	LEC (HP)	75	4		Contour plot (measurement sites on grid of 3 mm x 6 mm).
Skolnick et al.	J.Elect.Mat.	1/84	LEC (HP)	50	5		High resolution vidicon pictures
Skolnick et al.	A.P.L.	2/84	LEC (HP)	to 75	3		High resolution vidicon pictures
Holmes & Chen	J.A.P.	5/84	LEC (HP)	75	4		Contour plots based on measured 3 mm x 3 mm grid of locations
Duseaux & Martin	Kah-nee-ta,	1984	LEC (HP)	50	4	In-doped	Mosaic plot (1.5 mm resolution)
Osaka & Hoshikawa	" " "	1984	VMLEC (HP)	75	?	Magn. field	Radial line plot only
Foulkes et al.	" " "	1984	LEC (HP)	50	5	In-doped	Vidicon pictures, med-high res.
Rumsby et al.	" " "	1984	LEC (HP)	50	5	Annealed	Radial line trace only
Holmes et al.	" " "	1984	LEC (HP)	75	4	Incl.Anneal	Contour plots; 3 x 6 mm resolution
Leigh et al.	" " "	1984	LEC (HP & LP)	50	5	Incl.Anneal	High resolution vidicon pictures
Dobrilla et al.	" " "	1984	LEC (HP)	50	0.5 & 5		Mosaic plots (1 mm resolution)
Kaufmann et al.	" " "	1984	LEC	50	4		Vidicon images, medium resolution
Brozel et al.	" " "	1984	LEC	50	5		Line scan only
Skolnick et al.	" " "	1984	LEC	56	3		High-resolution vidicon pictures
Wang	" " "	1984	LEC (LP)	60	4		Line scan only, 4 mm resolution
Brown et al.	" " "	1984	LEC (HP)	50	3		Vidicon micrograph
Brozel et al.	J.A.P.	8/84	LEC (HP)	50	3 & 5		Line scans & vidicon pictures
Martin et al.	Biarritz	1985	LEC (HP)	50	4	In-doped	Mosaic plots before and after ingot anneal
Brozel et al.	Biarritz	1985	LEC (HP)	50	5		High-resolution vidicon micro-photos, attempt at stereo view.
Goutereaux et al.	Biarritz	1985	LEC (HP)	50	5		Mosaic plot, 1.5 mm resolution
Blakemore et al.	WOCSEMMAD	1985	LEC (HP)	50	0.5		Mosaic plot, 1 mm resolution, compared with device parameters
Dobrilla et al.	MRS/SFO	1985	LEC (HP)	50	0.5		Mosaic, 1 mm res., device comp.

Papers Reporting on the Spatial Variation over the area of a S.I. GaAs Wafer of Resistivity (or of "leakage current" test for intrinsic photosensitivity)

Authors	Published Conference or Journal	Publication Date	Type and size of Crystals used	Results reported
Blunt	Evian Conf.	1982	50 mm LEC and HB wafers	Contour map from "dark spot" response
Grant et al.	" "	1982	50 mm LEC (HP)	Contour map
Matsumura et al.	J.J.A.P.	3/83	50 mm LEC (HP)	Line scan (M-shape for ρ and photo-leakage)
Holmes et al.	A.P.L.	3/83	75 mm LEC (HP)	Line scans
Mita et al.	A.P.L.	11/83	50 mm LEC, & HB	Pseudo-3D plots, for photoresponse & leakage
Duseaux & Martin	Kah-nee-ta	1984	50 mm LEC, In-doped	Radial variation shown only
Rumsby et al.	" " "	1984	50 mm LEC, annealed	Line trace
Goutereaux et al.	Biarritz	1985	50 mm LEC (HP)	Mosaic plot of R_H (1.5 mm res.) compared with EL2

CONTINUATION

Feb. 1985 SUMMARY OF LITERATURE ON WAFER MAPS FOR S.I. GaAs

Papers Reporting on the Spatial Dependence of Dislocations over the Area of S.I. GaAs Wafers

Authors	Published Conference or Journal	Publication Date	Type and size of Crystals used	Results Reported
(a) Based on Etch Pit Counting				
Grant et al.	Evian Conf.	1982	50 mm LEC (HP)	Mosaic map display of EPD
Bonnet et al.	" "	1982	50 mm LEC (HP)	Mosaic map of EPD
Holmes et al.	A.P.L.	3/83	75 mm LEC (HP)	Radial line trace of EPD
Matsumura et al.	J.J.A.P.	3/83	50 mm LEC (HP)	Line scan of EPD
Mita et al.	A.P.L.	11/83	50 mm LEC & HB	Pseudo-3D plot of EPD
Holmes and Chen	J.A.P.	5/84	75 mm LEC (HP)	Contour maps of EPD
Ponce et al.	Kah-nee-ta	1984	LEC (prob. LP)	Line scan
Peigen et al.	" " "	1984	60 mm LEF (LP)	Line scan
DiLorenzo et al.	" " "	1984	LEC, incl. In-doped	Contour plot, and full-wafer photos
Stirland et al.	" " "	1984	LEC	High-magnification TEM compared with EPD.
Nakanishi et al.	ICSSDM, Kobe	1984	FEC, In-doped	Line scan
(b) Pictures and/or Traces from X-ray Topographs				
Brown et al.	Kah-nee-ta	1984	50 mm LEC (HP)	3 mm wafers used, slip bands shown
Ponce et al.	" " "	1984	LEC (prob. LP)	Transmission picture of full half-wafer
Leigh et al.	" " "	1984	50 mm LEC (HP)	0.3 mm wafers used for XRT, etc.
Strausser & Rosencwaig	" " "	1984	LEC	Thermal-wave image comp. with XRT for high-magn.

Papers Reporting on the Spatial Dependence across a S.I. GaAs Wafer of Carbon (& other shallow acceptors) as Deduced either from 17 μm Local Vibrational Mode (LVM) Absorption, or from near-bandgap Luminescence

Authors	Published Conference or Journal	Publication Date	Type and size of Crystals Used	Results Reported
Holmes et al.	Evian	1982	75 mm LEC (HP)	Radial line plot, from LVM absorption at 17 μm
Miyazawa et al.	A.P.L.	2/84	50 mm LEC	Room temp. cathodoluminescence, line scans with high resolution (∿2 μm).
Yokogawa et al.	J.J.A.P.	5/84	50 & 75 mm LEC	Mosaic plots of 4.2 K, 1.49 eV PL, 2 mm resolution
Duseaux and Martin	Kah-nee-ta	1984	50 mm LEC, In-doped	Reports uniform low carbon from LVM absorption
Kitihara et al.	" " "	1984	LEC and VPE layers	Line scans of PL at 1.494 eV (carbon) and at 1.490 eV (zinc) along (010) and (011) diameters
Leigh et al.	" " "	1984	50 mm LEC (HP)	4.2 K cathodoluminescence in SEM, with photos of 5 x 5 mm^2 samples, and detailed line scans at 1.514 eV (e-h, flat) and 1.494 eV (rugged)
Chin et al.	A.P.L.	9/84	LEC and HGF	300 K cathodoluminescence micrographs
Yokogawa et al.	Biarritz	1985	50 & 75 mm LEC	Mosaic plots of 1.49 eV PL showing anneal effects
Kikuta et al.	Biarritz	1985	Undoped S.I.(LEC?)	Microfocussed laser spot used to generate high resolution PL image at 1.49 eV, compare with the PL images for 0.65 eV and 0.8 eV.

Papers Reporting on Variation over a S.I. GaAs Wafer's area of Device Parameters (V_{th}, etc.)

Authors	Published Conference or Journal	Publication Date	Type and size of Crystals used	Results Reported
DiLorenzo et al.	Kah-nee-ta	1984	LEC, inc. In-doped	Mosaic plot of FET V_{th}
Takebe et al.	" " "	1984	75 mm LEC (Mod.P)	Mosaic plots for V_{th} and K
Lee et al.	" " "	1984	75 mm LEC (HP)	Pseudo-3D plots of V_{th} for FETs aligned along [010], [011], and [01$\bar{1}$] directions.
Winston et al.	" " "	1984	50 mm LEC, In-doped	Line plots of V_{th} for low-disloc. material
Yamazaki et al.	A.P.L.	11/84	50 mm LEC, In-doped	Mosaic plots of V_{th} for low disloc. mtl.
Winston et al.	Biarritz	1985	75 mm LEC, In-doped	Concerned with dislocation proximity in low-disloc. material as affecting V_{th} or CL.